A Generalized Higher Order Finite-Difference Time-Domain Method and Its Application in Guided-Wave Problems

Zhenhai Shao, Zhongxiang Shen, *Member, IEEE*, Qiuyang He, and Guowei Wei

***Abstract*—In this paper, a $(2M, 4)$ scheme of the finite-difference time-domain (FDTD) method is proposed, in which the time differential is of the fourth order and the spatial differential using the discrete singular convolution is of order $2M$. Compared with the standard FDTD and the scheme of (4, 4), the scheme of $(2M, 4)$ has much higher accuracy. By choosing a suitable $M \geq 2$, the $(2M, 4)$ scheme can arrive at the highest accuracy. In addition, an improved approximation of the symplectic integrator propagator is presented for the time differential. On one hand, it can directly simulate unlimited conducting structures without the air layer between the perfectly matched layer and inner structure; on the other hand, it needs only a quarter of the memory space required by the Runge–Kutta time scheme and requires one third of the meshes in every direction of the standard FDTD method. By choosing suitable meshes and bandwidth M, our scheme not only retains higher accuracy but also saves memory space and CPU time. Numerical examples are provided to show the high accuracy and effectiveness of proposed scheme.**

***Index Terms*—Discrete singular convolution (DSC), finite difference time domain (FDTD), Lagrange-delta kernel, symplectic integrator propagator.**

I. Introduction

THE finite-difference time-domain (FDTD) [1] method is a full-wave approach to the analysis of various electromagnetic problems, such as integrated transmission lines, discontinuities, scattering by intricate objects, and radiation from antennas. Although the FDTD method can analyze various electromagnetic problems, its accuracy is lower than integral methods. It is desirable to find a method that can not only retain the flexibility of the FDTD, but also achieve the higher accuracy of integral methods. During the past few years, many researchers have proposed a number of techniques to improve its accuracy. The scheme of (4, 4) was proposed by Young *et al.* [2], Zingg [3], Turkel and Yefet [4], based on the Runge–Kutta time scheme, and by Hirono *et al.* [5], [6], using the symplectic integrator propagator, which is basically a time-integration method for Hamiltonian systems [7], [8]. However, it has been observed that these schemes of (4, 4) cannot increase the accuracy significantly. More importantly, these schemes [5], [6] cannot directly extend conductors to the perfectly matched layer (PML) boundary. In order to include conductors in the PML boundary for the Runge–Kutta time scheme, the PML condition must be treated specially [9].

In this paper, a generalized FDTD method based on the $(2M, 4)$ scheme is presented using the discrete singular convolution (DSC) and symplectic integrator propagator, where M is the bandwidth. The DSC algorithm was proposed as a potential approach for the computer realization of singular integrations. The theory of distribution and wavelet analysis form the mathematical foundation for the DSC. Compared to the multiresolution time-domain (MRTD) method [10], the expression of arbitrary bandwidth M for spatial differential can be obtained more easily. By choosing a suitable M, the scheme of $(2M, 4)$ can achieve higher accuracy than the standard FDTD method and the scheme of (4, 4) [2]. By choosing the symplectic integrator propagator as the time-domain scheme, the scheme $(2M, 4)$ requires much less memory than the standard FDTD method and the scheme of (4, 4) in [2].

This paper is organized as follows. In Section II, the DSC method based on the Lagrange delta kernel (LK) is introduced. An improved symplectic integrator propagator scheme is proposed in Section III. In Section IV, using the generalized FDTD scheme, several numerical examples for two-dimensional (2-D) and three-dimensional (3-D) guided-wave problems are analyzed and the performance of the $(2M, 4)$ scheme is also discussed.

II. Spatial Discretization

A. The DSC Method

Let T be a distribution and $f(x)$ be an element of the space of test functions. The singular convolution of $f(x)$ is defined as

$$F(t) = (T * f)(t) = \int_{-\infty}^{+\infty} T(t - x) f(x)\, dx. \tag{1}$$

Its DSC can be written as

$$F_\alpha(t) = \sum_i T_\alpha(t - x_i) f(x_i) \tag{2}$$

where T_α is the sequence of approximations to T, F_α is an approximation to $F(t)$, and $\{x_i\}$ is a set of discrete points.

Unlike the standard FDTD method [1], in which the center difference for space and time differential is used, the DSC method [11] is used to discretize the spatial difference. When

Manuscript received January 27, 2002; revised September 19, 2002.

Z. Shao and Z. Shen are with the School of Electrical and Electronic Engineering, Nanyang Technological University, Singapore 639798; (e-mail: ezhshao@ntu.edu.sg).

Q. He is with the Department of Information Engineering, Nanjing University of Posts and Telecommunications, Nanjing 210003, China.

G. Wei was with the Department of Computational Science, National University of Singapore, Singapore 117543. He is now with the Department of Mathematics, Michigan State University, East Lansing, MI 48823 USA.

Digital Object Identifier 10.1109/TMTT.2003.808627

the standard Yee's cell is used, the nth-order spatial differentiation of the electromagnetic field function f by the DSC method can be shown as follows:

$$f^{(n)}(x) = \sum_{k=-M}^{-1} \delta_{\sigma,\Delta}^{(n)}(x - x_{k+1/2}) f(x_{k+1/2}) + \sum_{k=1}^{M} \delta_{\sigma,\Delta}^{(n)}(x - x_{k-1/2}) f(x_{k-1/2}) \quad (3)$$

where $\delta_{\sigma,\Delta}^{(n)}(x-x_k) = (d/dx)^n \delta_{\sigma,\Delta}(x-x_k)$, $\delta_{\sigma,\Delta}(x-x_k)$ is the DSC delta kernel, and M is the bandwidth. There are many delta kernels, such as Shannon's delta kernel, the LK, and Posisson's delta kernel. In this paper, only the LK is considered. Compared with other delta kernels, the LK needs less bandwidth for the same accuracy.

It is well known that the LK is given as

$$L_{M,k}(x) = \prod_{i=k-M, i\neq k}^{k+M} \frac{x - x_i}{x_k - x_i}. \quad (4)$$

Its regularized form is

$$\delta_\sigma(x - x_k) = \left[\prod_{i=k-M, i\neq k}^{k+M} \frac{x - x_i}{x_k - x_i} \right] e^{-\frac{(x-x_k)^2}{2\sigma^2}}. \quad (5)$$

The LK of order n and bandwidth M can be computed by a recurrence method [12].

For $n = 1$, using the Taylor's expansion and considering the characteristic of the Lagrange polynomial (4), the error term R_{LK} of the LK (4) can be derived as

$$R_{\mathrm{LK}} \propto \frac{[(2M-1)!!]^2}{(2M+1)!} O\left(\left(\frac{\Delta x}{2} \right)^{2M} \right). \quad (6)$$

B. Boundary Conditions

As the DSC kernels are either symmetric or antisymmetric, they require approximating the function values outside the computational domain. Therefore, the following boundary conditions can be used.

For a perfect electric wall, the tangential electric field E_t and the normal magnetic field H_n outside the computational domain are obtained by antisymmetric extensions, whereas, for the normal electric field E_n and the tangential magnetic field H_t, symmetric extensions are used.

For a perfect magnetic wall, the tangential magnetic field H_t and the normal electric field E_n outside the computational domain are obtained by antisymmetric extensions, whereas, for the normal magnetic field H_n and the tangential electric field E_t, symmetric extensions are used.

For a periodic boundary, all electric and magnetic fields outside the computational domain are obtained by periodic extensions.

For an open boundary, the PML condition can be used to determine field values outside the computational domain.

III. Improved PML Condition With Pade Approximation

In this paper, the PML condition based on the symplectic integrator propagator [5], [6] is introduced to truncate the open boundary. However, it is found that the PML condition based on the symplectic integrator propagator in [5] and [6] cannot be used to truncate unlimited conductor boundary directly.

In [5] and [6], a 3-D fourth-order FDTD scheme using a symplectic integrator propagator was proposed. Its basic idea is briefly reviewed here for clarity.

Maxwell's equations in an isotropic and source-free medium are written in a matrix form as

$$\frac{\partial}{\partial t} \begin{pmatrix} H \\ E \end{pmatrix} = W \begin{pmatrix} H \\ E \end{pmatrix} \quad (7)$$

where

$$W = \begin{pmatrix} -\mu^{-1}\sigma^* I_3 & -\mu^{-1} R \\ \varepsilon^{-1} R & -\varepsilon^{-1}\sigma I_3 \end{pmatrix} = U + V \quad (8)$$

$$U = \frac{1}{\mu} \begin{pmatrix} -\sigma^* I_3 & -R \\ 0 & 0 \end{pmatrix},$$

$$V = \frac{1}{\varepsilon} \begin{pmatrix} 0 & 0 \\ R & -\sigma I_3 \end{pmatrix}. \quad (9)$$

The solution after a time step Δ_t is expressed by the exponential operator $\exp(\Delta_t W)$ as

$$\begin{pmatrix} H \\ E \end{pmatrix} (\Delta_t) = \exp(\Delta_t W) \begin{pmatrix} H \\ E \end{pmatrix} (0) \quad (10)$$

where $\exp(\Delta_t W)$ is approximated by the symplectic integrator propagator, which is the multiproduct of the exponential operator of U and of V. The propagator approximates $\exp(\Delta_t W)$ as

$$\exp(\Delta_t W) = \prod_{p=1}^{m} \exp(d_p \Delta_t V) \exp(c_p \Delta_t U) + O((\Delta_t)^{n+1}) \quad (11)$$

where c_p and d_p are real coefficients characterizing the propagator [5], [6], n is the order of the approximation, and m is the stage number of the propagator

$$\exp(\Delta_t U) = \begin{pmatrix} \exp\left(-\frac{\Delta_t \sigma^*}{\mu}\right) I_3 & -\frac{1-\exp\left(\frac{-\Delta_t \sigma^*}{\mu}\right)}{\sigma^*} R \\ \{0\} & I_3 \end{pmatrix} \quad (12)$$

$$\exp(\Delta_t V) = \begin{pmatrix} I_3 & \{0\} \\ \frac{1-\exp(-\Delta_t \sigma/\varepsilon)}{\sigma} R & \exp\left(-\frac{\Delta_t \sigma}{\varepsilon}\right) I_3 \end{pmatrix}. \quad (13)$$

In [5] and [6], the following exponential functions are approximated by Padé's approximation of (2, 2):

$$\exp(-w) \approx \frac{1 - w/2 + w^2/12}{1 + w/2 + w^2/12} \quad (14)$$

$$\frac{1 - \exp(-w)}{w} \approx \frac{1 - w/10 + w^2/60}{1 + 2w/5 + w^2/20} \quad (15)$$

where $w = \Delta_t \sigma/\varepsilon$ or $w = \Delta_t \sigma^*/\mu$.

In this paper, the quadratic profile of conductivity $\sigma(\rho) = \sigma_m(\rho/\delta)^n$ [13], [14] is chosen. So, the reflection factor for a PML of thickness δ is

$$R(\theta) = \exp\left(-\frac{2}{n+1}\frac{\sigma_m\delta}{\varepsilon c}\cos(\theta)\right) \tag{16}$$

where ε is the dielectric constant, c is the vacuum velocity, and θ is the angle of incidence. By choosing $\theta = 0^o$, σ_m can be obtained from (16) as

$$\sigma_m = -\frac{(n+1)\varepsilon c \ln R_m}{2\delta}. \tag{17}$$

When the spatial increment Δh and the time increment Δt are chosen, the conductivities at the mesh points are implemented as the average value in the cell around the index location. At index l, we have

$$\begin{aligned}\sigma(l) &= \frac{1}{\Delta h}\int_{l\cdot\Delta h-\Delta h/2}^{l\cdot\Delta h+\Delta h/2}\sigma_m\left(\frac{\rho}{\delta}\right)\\ &= \frac{\delta\cdot\sigma_m}{\Delta h}\frac{1}{n+1}\left[\left(\frac{l+0.5}{N}\right)^{n+1}-\left(\frac{l-0.5}{N}\right)^{n+1}\right]\\ &= \frac{\delta\cdot\sigma_m}{\Delta h}\frac{1}{n+1}\cdot f(l)\end{aligned} \tag{18}$$

where $\delta = N\cdot\Delta h$.

In order to satisfy the stability condition, we choose the time increment as

$$\Delta t = \frac{\Delta h}{\beta\cdot c} \tag{19}$$

where β is usually greater than 1 for most planar circuit problems. If Δh is the minimum space increment in (19), then $\beta > \sqrt{2M}$ for 2-D propagation problems and $\beta > \sqrt{3M}$ for 3-D propagation problems,

From (17)–(19), we can obtain

$$\frac{\sigma(l)\cdot\Delta t}{\varepsilon} = -\frac{\ln(R_m)}{2\beta}f(l) < -\frac{\ln(R_m)}{2\beta} \tag{20}$$

where the condition $\sigma/\varepsilon = \sigma^*/\mu$ was invoked for low-loss media. It is seen from (20) that $(\sigma/\varepsilon)\Delta t$ is smaller than $-\ln(R_m)/2$. Normally, when $10^{-10} \le R_m \le 10^{-6}$ for most microstrip circuit problems, $(\sigma/\varepsilon)\Delta t$ is smaller than 12 for lossless and low-loss dielectric media. However, in good conductor and high-loss media ($\sigma \gg \omega\varepsilon$), the value of $(\sigma/\varepsilon)\Delta t$ can be very big.

Fig. 1 shows the comparison between the right-hand side of (14) and $\exp(-w)$. It is obvious that, when w is small, the right-hand side of (14) is a good approximation to $\exp(-w)$ However, when w is large, the right-hand side of (14) can not approximate $\exp(-w)$ well.

Fig. 2 shows the comparison between the right-hand side of (15) and $(1-\exp(-w))/w$. It is seen that, when w is small, the right-hand side of (15) is a good approximation to $(1-\exp(-w))/w$. Similarly, when w is large, the right-hand side of (15) cannot approximate $(1-\exp(-w))/w$ well.

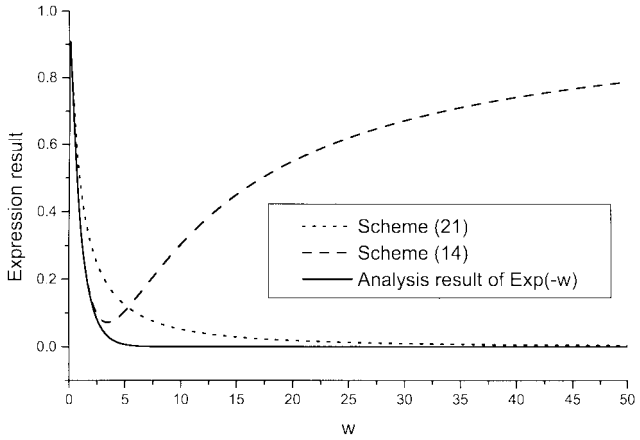

Fig. 1. Comparison between two kinds of approximation for $\exp(-w)$.

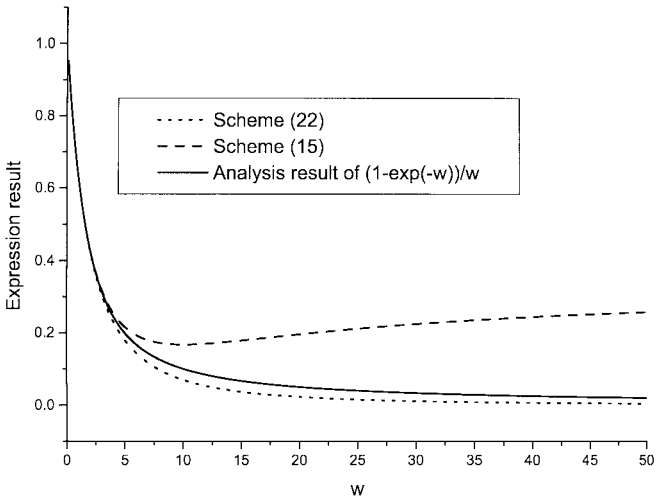

Fig. 2. Comparison between two kinds of approximation for $[1-\exp(-w)]/w$.

Because $\sigma \gg \omega\varepsilon$ for a good conductor, $(\sigma/\varepsilon)\Delta t$ is very large. Therefore, in the FDTD, (14) and (15) cannot be used for a conductor and extend an unlimited conductor to the PML condition, such as in 3-D microstrip problems. Here, improved approximations are presented according to Padé's approximation of (0, 2)

$$\exp(-w) \approx \frac{1}{1+w+w^2/2} \tag{21}$$

$$\frac{1-\exp(-w)}{w} \approx \frac{1}{1+w/2+w^2/12}. \tag{22}$$

From Fig. 1, it is seen that, when w is small, (21) can give an acceptable approximation to $\exp(-w)$. However, when w increases, (21) gives a better approximation to $\exp(-w)$ than (14) does. The similar comparison between (15) and (22) is shown in Fig. 2. In the entire range, (22) has a better approximation to $(1-\exp(-w))/w$ than (16).

Combining (3), (12), (13), (21), and (22) with (11), the scheme of the $(2M,4)$ FDTD method can be constructed. If $M = 2$ and the PML scheme uses (14) and (15), the $(2M,4)$ scheme reduces to the fourth-order FDTD scheme using a symplectic integrator propagator [5], [6]. If $M = 1$ and the central difference for the first-order time differentiation is used, it becomes the standard FDTD method.

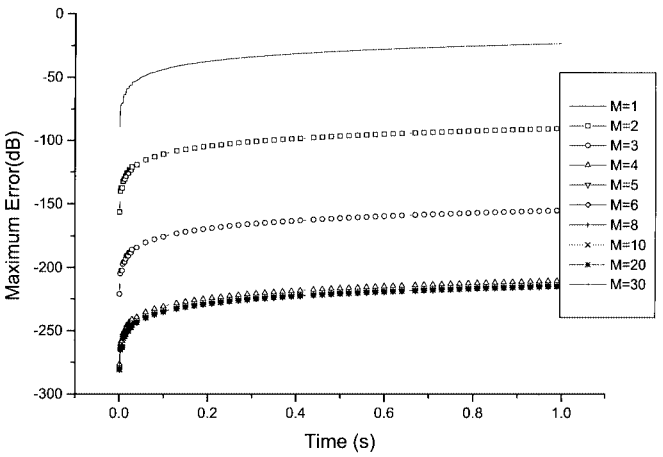

Fig. 3. Variation of the maximum error for different bandwidths for $\Delta t = 0.0001/c_0$.

TABLE I
MAXIMUM ERROR AND CPU TIME FOR DIFFERENT MESHES IN EVERY DIRECTION BY THE STANDARD FDTD METHOD

Meshes	Maximum error (dB)	CPU time (s)
25	-11.590	136
50	-23.861	499
100	-37.162	1966

TABLE II
MAXIMUM ERROR AND CPU TIME FOR DIFFERENT MESHES IN EVERY DIRECTION AND DIFFERENT BANDWIDTHS BY THE $(2M, 4)$ SCHEME

Meshes	Bandwidth (M)	Maximum error (dB)	CPU time (s)
5	2	-11.632	28
5	3	-36.436	32
5	4	-60.130	39
5	5	-83.154	44
10	2	-34.661	87
10	3	-71.375	103
10	4	-106.933	124
10	5	-141.807	137
25	1	-11.497	675
50	1	-23.479	856
50	6	-214.742	3456

IV. EXAMPLES

To illustrate the application of the proposed $(2M, 4)$ scheme to electromagnetic wave problems, a 2-D air-filled rectangular waveguide is first considered. The waveguide length and width are both 0.01 m and the cross section is discretized by 51×51 grid points. M is chosen from 1 to 30, and $f = 23.9769$ GHz. For every fixed M, the DSC parameters $\{\delta^{(1)}_{\sigma,\Delta}\}$ can be obtained by the recurrence method starting from $M = 1$. In order to eliminate the error introduced by the time increment, Δt is chosen to be very small $(0.00001/c)$. Fig. 3 shows the maximum error between analytical results and numerical results for different values of M. The maximum error is defined as

$$\max_{(x,y)\in\Omega} |f_N - f_A|(x, y)$$

where f_N is the numerical field value, f_A is the analytical field value, and Ω is the interior domain.

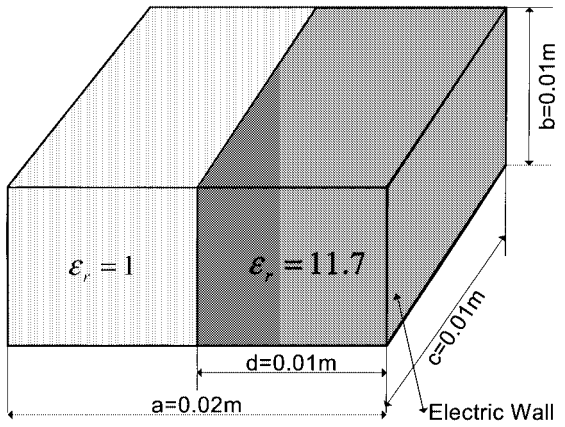

Fig. 4. Geometry of a rectangular waveguide partially loaded with a dielectric slab.

TABLE III
COMPARISON OF CUTOFF FREQUENCY RESULTS (GIGAHERTZ) FROM DIFFERENT SCHEMES OF THE FDTD METHOD

Analytical result (GHz)	R_e of scheme (14) and (15) (dB)	R_e of scheme (21) and (22) (dB)	Standard FDTD (dB)
16.0218	-63.507	-63.507	-57.325
19.7099	-65.553	-67.503	-55.037
21.6386	-61.267	-61.267	-52.536
24.7317	-64.519	-64.519	-47.302
28.6893	-63.354	-63.354	-44.842
32.2307	-57.888	-57.888	-45.031
34.4280	-55.175	-55.175	-44.605
37.7809	-64.697	-63.977	-39.379
41.7686	-44.344	-44.344	-38.551
47.9226	-56.5	-56.746	-39.675
51.0020	-60.401	-60.069	-34.929

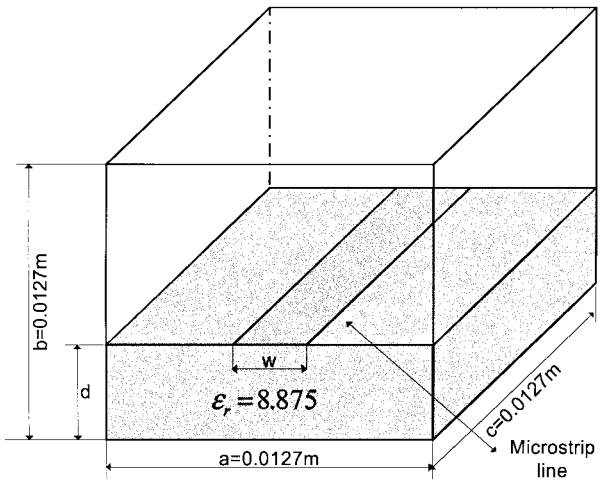

Fig. 5. Geometry of a shielded microstrip line, where $d = w = 0.00127$ m.

It is seen that when M varies from 1 to 4, the maximum error will decrease about 65 dB for every increment of M. This result is in agreement with (6). Therefore, we can choose a suitable

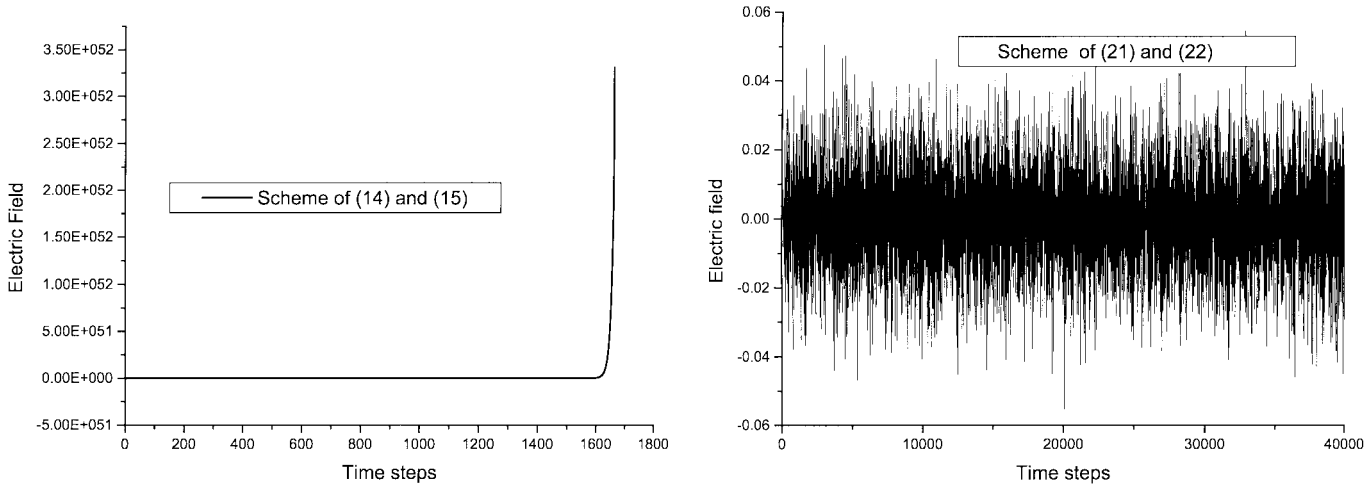

(a) (b)

Fig. 6. Comparison of time-domain electric field results at node (5,5,5) between: (a) the scheme of (14) and (15) and (b) the scheme of (21) and (22).

M from (6) according to the required accuracy. However, when M is bigger than 4, the maximum error almost keeps constant. In the examples that follow, $M = 6$ is used to obtain a higher accuracy.

Tables I and II compare the maximum error (for $t = 1$ s) and CPU time between the $(2M, 4)$ scheme and the standard FDTD method. If using the same mesh in every direction, the $(2M, 4)$ scheme needs more CPU time than the standard FDTD for any bandwidth M. It is seen from Table II that, for the same meshes, the $(2M, 4)$ scheme can achieve a higher accuracy with a slight increase in CPU time by increasing the bandwidth M. However, If choosing much smaller meshes $(1/3$–$1/10)$ in every direction and a larger bandwidth $M \geq 2$, the $(2M, 4)$ scheme can obtain a higher accuracy with less CPU time.

The second example is a rectangular waveguide partially loaded with a slab of dielectric material [15], as shown in Fig. 4. This problem is selected to verify that the improved scheme of (21) and (22) has the same accuracy as that of (14) and (15) for lossless dielectric media. Meshes are chosen to be $N_x = 50$, $N_y = N_z = 25$, and $\Delta t = 0.0001/c_0$. Two PML conditions are added in the z direction to terminate the computational domain. $R(0)$ is 10^{-6}, $N = 10$, and the factor n in the conductivity relation (17) is 3. Table III shows the comparative results of the cutoff frequencies from the standard FDTD method, the scheme of (14) and (15), and the scheme of (21) and (22). From the table, it is seen that the scheme of (21) and (22) produces the same results as the scheme of (14) and (15). For every TM mode, the DSC method has very lower relative errors R_e(20log(|analytical result-numerical result|/analytical result)) than the standard FDTD method, and the difference between them is from 6 to 25 dB.

The determination of mode cutoff frequencies based on the time-domain DSC method and the improved PML is generalized to a shielded microstrip line, as shown in Fig. 5. This problem is slightly more complicated than the previous two examples and it does not have an exact solution. The strip line is assumed to be a good conductor with parameters $\varepsilon_r = 1$, $\mu_r = 1$, and $\sigma = 2. \times 10^6$ S/m.

TABLE IV
COMPARISON OF CUTOFF FREQUENCY RESULTS (GIGAHERTZ) BETWEEN OUR RESULTS AND THOSE OBTAINED BY HFSS

Results of (2M, 4) scheme	HFSS Results
16.93875	16.8977
22.56698	22.7337
23.46411	23.5520
27.70574	27.6291
29.33492	29.3668

The interior region of the square cross section is discretized into many small square cells $N_x = N_y = N_z = 51$ and the time increment is $\Delta t = 0.0001/c_0$. In order to excite every possible mode in the cavity-type structure, the following electric field distribution is used [15] in the transverse face:

$$E_z = \exp\left\{-\frac{(x-x_c)^2+(y-y_c)^2}{2\tau^2}\right\}, \qquad \text{for } z > z_c \quad (23)$$

where (x_c, y_c, z_c) is the center node of interior domain.

Fig. 6 shows the comparison of the scheme (21) and (22) with the scheme (14) and (15). It is obvious that the solution of the scheme of (14) and (15) diverges after 1600 time steps. However, the solution of the scheme of (21) and (22) is very stable in all calculated time steps. Therefore, it can be concluded that the scheme (21) and (22) can deal with conductor problems very well.

Table IV shows the comparison of the cutoff frequencies calculated by the DSC method based on an improved symplectic scheme and those obtained by Ansoft's High-Frequency Structure Simulator (HFSS). It is seen that they are in good agreement. Therefore, the improved symplectic scheme can be used to extend conductors to the PML boundary directly without any modification.

V. Conclusion

In this paper, a generalized time-domain higher order finite-difference method, based on the LK of DSC (TD-DSC) algorithm, and a modified PML absorbing boundary condition, is introduced to analyze 3-D guided-wave problems. The presented scheme has the same flexibility as the standard FDTD method in handling homogeneous and inhomogeneous microwave problems. Its accuracy can be much higher than the standard FDTD method by choosing a suitable bandwidth. The higher order Langrage scheme can achieve a satisfactory accuracy with three to six points per wavelength, whereas the standard FDTD scheme usually requires 12–18 points per wavelength. Due to its high accuracy, the higher order Langrage method is more efficient than the standard FDTD method for a given simulation, though this scheme requires a longer computational time than the standard FDTD method over a given grid. Based on the symplectic integrator propagator and its improved approximation, the higher order Langrage method requires not only less memory than the standard FDTD method and the scheme of (4, 4), but the PML condition can also be extended to directly truncate microstrip lines. Therefore, the combination of the higher order Langrage scheme and the modified PML absorbing boundary condition provides improvements in memory saving and achieving higher accuracy.

References

[1] K. S. Yee, "Numerical solution of initial boundary value problems involving Maxwell's equations in isotropic media," *IEEE Trans. Antennas Propagat.*, vol. AP-14, pp. 302–307, May 1966.

[2] J. L. Young, D. Galitonde, and J. J. S. Shang, "Toward the construction of a fourth-order difference scheme for transient EM wave simulation: Staggered grid approach," *IEEE Trans. Antennas Propagat.*, vol. 45, pp. 1573–1580, Nov. 1997.

[3] D. W. Zingg, "Higher-order finite-difference methods in computational electromagnetics," in *IEEE AP-S Int. Symp. Dig.*, Montreal, QC, Canada, 1997, pp. 110–113.

[4] E. Turkel and A. Yefet, "Fourth order method for Maxwell's equations on a staggered mesh," in *IEEE AP-S Int. Symp.*, Montreal, QC, Canada, 1997, pp. 2156–2159.

[5] T. Hirono, W. Lui, S Seki, and Y. Yoshikuni, "A three-dimensional fourth-order finite-difference time-domain scheme using a symplectic integrator propagator," *IEEE Trans. Microwave Theory Tech*, vol. 49, pp. 1640–1647, Sept. 2001.

[6] T. Hirono, W. W. Lui, and S. Seki, "Successful application of PML-ABC to the symplectic FDTD scheme with 4th-order accuracy in time and space," in *IEEE MTT-S Int. Microwave Symp. Dig.*, Anaheim, CA, 1999, pp. 1293–1296.

[7] E. Hairer, S. P. Nrsett, and G. Wanner, *Solving Ordinary Differential Equations I*. Berlin, Germany: Springer-Verlag, 1992.

[8] J. M. Sanz-Serna and M. P. Calvo, *Numerical Hamiltonian Problems*. London, U.K.: Chapman & Hall, 1994.

[9] T. Li, W. Sui, and M. Zhou, "Extending PML absorbing boundary condition to truncate microstrip line in nonuniform 3-D FDTD grid," *IEEE Trans. Microwave Theory Tech.*, vol. 47, pp. 1771–1776, Sept. 1999.

[10] M. Krumpholz and L. P. B. Katehi, "MRTD: New time-domain schemes based on multiresolution analysis," *IEEE Trans. Microwave Theory Tech.*, vol. 44, pp. 555–571, Jan. 1996.

[11] G. W. Wei, "Discrete singular convolution for the solution of the Fokker-Planck equations," *J. Chem. Phys.*, vol. 110, pp. 8930–8942, 1999.

[12] B. Fornberg, *A Practical Guide to Pseudospectral Methods*. Cambridge, U.K.: Cambridge Univ. Press, 1996.

[13] J. P. Berenger, "A perfectly matched layer for the absorption of electromagnetic waves," *J. Comput. Phys.*, vol. 114, no. 2, pp. 185–200, Oct. 1994.

[14] ——, "Perfectly matched layer for the FDTD solution of wave-structure interaction problems," *IEEE Trans. Microwave Theory Tech.*, vol. 44, pp. 110–117, Jan. 1996.

[15] S. M. Rao, *Time Domain Electromagnetics*. New York: Academic, 1999, ch. 6.

Zhenhai Shao was born in Jiangsu, China, on December 1, 1971. He graduated from the Nanjing Normal University of China, Nanjing, China, in 1994. He received the M.S. and Ph.D. degrees from the Southeast University of China, Najing, China, in 1997 and 2000, respectively.

From 2000 to 2001, he was with the National University of Singapore. He is currently a Research Fellow with the Department of Electric and Electronic Engineering, Nanyang Technological University of Singapore. He has authored approximately 20 technical publications. His research interests include the design and simulation of package of monolithic microwave integrated circuits (MMICs) and planar microwave circuits, numerical procedures of FDTD, transmission-line matrix (TLM), time-domain finite-element method (TDFEM), and the DSC method for passive microwave components and software design.

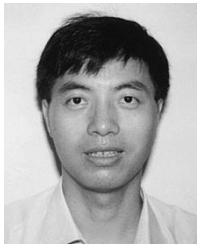

Zhongxiang Shen (S'96–M'99) was born in Zhejiang Province, China, in July 1966. He received the B.E. degree from the University of Electronic Science and Technology of China, Chengdu, China, in 1987, the M.S. degree from Southeast University, Nanjing, China, in 1990, and the Ph.D degree from the University of Waterloo, Waterloo, ON, Canada, in 1998, all in electrical engineering, respectively.

From 1990 to 1994, he was with Nanjing University of Aeronautics and Austronautics, Nanjing, China. From 1994 to 1997, he was a Graduate Research and Teaching Assistant with the Department of Electrical and Computer Engineering, University of Waterloo. He was with Com Dev Ltd., Cambridge, ON, Canada, for eight months as an Advanced Member of Technical Staff in 1997. He spent six months each in 1998, first with the Gordon McKay Laboratory, Harvard University, Cambridge, MA, and then with the Radiation Laboratory, The University of Michigan at Ann Arbor, as a Post-Doctoral Fellow. He is currently an Assistant Professor with the School of Electrical and Electronic Engineering, Nanyang Technological University, Singapore. His research interests are microwave/millimeter-wave passive devices and circuits, small and planar antennas for wireless communications, and numerical modeling of various RF/microwave components and antennas. He authored over 70 papers published in international journals and conference proceedings.

Dr. Shen was the recipient of a Post-Doctoral Fellowship presented by the Natural Sciences and Engineering Research Council of Canada. He was also the recipient of the Third-Place Award in the Student Paper Competition at the 1997 IEEE Antennas and Propagation Society (AP-S) International Symposium.

Qiuyang He was born in Henan Province, China, in September 1971. She received the B.E. degree from the East China Normal University. Shanghai, China.

From 1994 to 2000, she was a Teacher with the Posts and Telecommunications School, Jiangsu Province, China. She is currently a Lecturer with the Department of Information Engineering, Nanjing University of Posts and Telecommunications, Nanjing, China.

Guowei Wei received the Ph.D. degree from the University of British Columbia, Victoria, BC, Canada, in 1996.

He was a Natural Sciences and Engineering Research Council of Canada (NSERC) Post-Doctoral Fellow and Research Assistant Professor with the University of Houston prior to joining the Department of Computational Science, National University of Singapore, Singapore, in 1998, where he was an Assistant/Associate Professor. Since 2002, he has been an Associate Professor with the Department of Mathematics, Michigan State University, East Lansing. His research interests include computational methodology and its applications, image processing, and nonlinear dynamics.